HHS Public Access

Author manuscript

J Immunol. Author manuscript; available in PMC 2018 February 15.

Published in final edited form as:

J Immunol. 2017 February 15; 198(4): 1616–1626. doi:10.4049/jimmunol.1601770.

Widespread virus replication in alveoli drives acute respiratory distress syndrome in aerosolized H5N1 influenza infection of macaques[1]

Elizabeth R. Wonderlich[*,†], **Zachary D. Swan**[*,†], **Stephanie J. Bissel**[‡], **Amy L. Hartman**[*,†], **Jonathan P. Carney**[§], **Katherine J. O'Malley**[*,¶], **Adebimpe O. Obadan**[‖], **Jefferson Santos**[‖], **Reagan Walker**[#], **Timothy J. Sturgeon**[*], **Lonnie J. Frye Jr**[**,†], **Pauline Maiello**[**], **Charles A. Scanga**[**], **Jennifer D. Bowling**[*,†], **Anthea L. Bouwer**[*,†], **Parichat A. Duangkhae**[*,†], **Clayton A. Wiley**[‡], **JoAnne L. Flynn**[**], **Jieru Wang**[††], **Kelly S. Cole**[*,¶], **Daniel R. Perez**[‖], **Douglas S. Reed**[*,¶], and **Simon M. Barratt-Boyes**[*,†,¶,2]

[*]Center for Vaccine Research, University of Pittsburgh, Pittsburgh, Pennsylvania, United States of America

[†]Department of Infectious Diseases and Microbiology, University of Pittsburgh Graduate School of Public Health, Pittsburgh, Pennsylvania, United States of America

[‡]Department of Pathology, Division of Neuropathology, University of Pittsburgh School of Medicine, Pittsburgh, Pennsylvania, United States of America

[§]Department of Radiology, University of Pittsburgh School of Medicine, Pittsburgh, Pennsylvania, United States of America

[¶]Department of Immunology, University of Pittsburgh School of Medicine, Pittsburgh, Pennsylvania, United States of America

[‖]Department of Population Health, University of Georgia, Athens, Georgia, United States of America

[#]Division of Laboratory Animal Resources, University of Pittsburgh, Pittsburgh, Pennsylvania, United States of America

[**]Department of Microbiology and Molecular Genetics, University of Pittsburgh School of Medicine, Pittsburgh, Pennsylvania, United States of America

[††]Department of Pediatrics, Division of Pulmonary Medicine, Allergy and Immunology, University of Pittsburgh School of Medicine, Pittsburgh, Pennsylvania, United States of America

Abstract

Human infections with highly pathogenic avian influenza A (H5N1) virus are frequently fatal but the mechanisms of disease remain ill-defined. H5N1 infection is associated with intense production of proinflammatory cytokines, but whether this cytokine storm is the main cause of

[1]This work was supported by funds from the University of Pittsburgh (SMBB) and the University of Georgia (DRP) and by the National Institutes of Health grant AI111598 (SJB and CAW) and contract HHSN272201400008C (DRP).

[2]Address correspondence and reprint requests to Dr. Simon M. Barratt-Boyes, University of Pittsburgh, 3501 Fifth Avenue, 9046 Biomedical Science Tower 3, Pittsburgh, PA 15261. Tel: 412-383-7537, Fax: 412-624-4440, smbb@pitt.edu.

fatality or is a consequence of extensive virus replication that itself drives disease remains controversial. Conventional intratracheal inoculation of a liquid suspension of H5N1 influenza virus in nonhuman primates likely results in efficient clearance of virus within the upper respiratory tract and rarely produces severe disease. We reasoned that small particle aerosols of virus would penetrate the lower respiratory tract and blanket alveoli where target cells reside. We show that inhalation of aerosolized H5N1 influenza virus in cynomolgus macaques results in fulminant pneumonia that rapidly progresses to acute respiratory distress syndrome with a fatal outcome reminiscent of human disease. Molecular imaging revealed intense lung inflammation coincident with massive increases in proinflammatory proteins and interferon-α in distal airways. Aerosolized H5N1 exposure decimated alveolar macrophages, which were widely infected and caused marked influx of interstitial macrophages and neutrophils. Extensive infection of alveolar epithelial cells caused apoptosis and leakage of albumin into airways, reflecting loss of epithelial barrier function. These data establish inhalation of aerosolized virus as a critical source of exposure for fatal human infection and reveal that direct viral effects in alveoli mediate H5N1 disease. This new nonhuman primate model will advance vaccine and therapeutic approaches to prevent and treat human disease caused by highly pathogenic avian influenza viruses.

Introduction

Human infection with highly pathogenic avian influenza A viruses of the H5N1 subtype is characterized by severe pneumonia that frequently progresses to acute respiratory distress syndrome and death (1). Since its re-emergence in 2003 there have been more than 850 confirmed cases of human H5N1 infection worldwide with a cumulative case fatality rate of more than 50%. The virus is an emerging global health threat, with 173 confirmed human cases in Egypt in 2014-2015 associated with widespread H5N1 infection in poultry (www.who.int/influenza/human_animal_interface/en/). Highly pathogenic avian H5 viruses were detected in the United States for the first time in 2014 and caused widespread outbreaks and death in poultry (2), although these viruses currently present a low risk for animal-to-human transmission (3).

The pathogenesis of human H5N1 pneumonia and the relative contribution of virus replication and immunopathology in driving disease remain unclear, and this has fundamental implications in how we treat severe H5N1 infections. H5N1 virus infects human alveolar epithelial cells (AEC) (4–9), and loss of alveolar barrier function through AEC death (6, 10) could be a central factor in progressive H5N1 pneumonia. H5N1 also binds to and infects alveolar macrophages in the human lower respiratory tract (4, 8). Alveolar macrophages play a critical role in protecting the lung from damage (11), but the impact of highly pathogenic H5N1 infection on alveolar macrophage survival *in vivo* has not been evaluated. Markedly increased plasma levels of proinflammatory cytokines and chemokines including IP-10 (CXCL10), MCP-1 (CCL2), and IL-6 are a hallmark of human H5N1 infection (12–15). H5N1 induces more profound cytokine responses from AEC and macrophages *in vitro* than less pathogenic isolates (13, 16–18), supporting the hypothesis that a harmful cytokine storm is central to disease pathogenesis (17, 19). However, whether proinflammatory cytokines drive disease or are a consequence of virus replication that itself damages the lung remains controversial (20).

Studies in nonhuman primates have substantially advanced our understanding of human infection with highly pathogenic H5N1 viruses largely through genome- and transcriptome-based analyses but have not addressed the cellular factors mediating disease (21–26). A significant issue with nonhuman primate studies to date is that unlike human disease, infection causes death in only a small minority of animals (21–23, 26). All published nonhuman primate studies have used an inoculation method involving application of virus in liquid suspension (21–26) or via large droplets (27) into the trachea, often in combination with other mucosal routes. These delivery methods are unlikely to expose target cells in the alveoli to significant quantities of virus because liquid suspensions and/or large droplets are cleared by the mucociliary apparatus of the upper respiratory tract. In contrast, small-particle aerosols of virus of 5 um or less in diameter remain in suspension in air for sustained periods of time and penetrate to the lower respiratory tract when inhaled (28, 29). Studies in the ferret model show that aerosol inoculation resembles a natural, airborne infection with H5N1 virus that is highly infectious and lethal (30, 31); however this route of exposure has not been attempted in nonhuman primates.

In this study we explored the use of small-particle aerosols in H5N1 infection of macaques. We report that infection with aerosolized influenza A/Vietnam/1203/2004 (H5N1) virus causes fulminant pneumonia that rapidly progresses to the acute respiratory distress syndrome, recapitulating fatal human disease. Our data indicate that direct damage to the alveolus is the central factor in disease pathogenesis, as widespread infection of cells in the alveoli leads to massive alveolar macrophage depletion and AEC apoptosis that significantly compromises the crucial barrier function of the alveolus. Our findings indicate that aerosolized H5N1 virus blankets target cells in alveoli and is likely a major and unappreciated source of exposure in fatal human infections. The work establishes a new nonhuman primate disease model for evaluation of vaccine and therapeutic approaches to prevent and treat infection with highly pathogenic avian influenza viruses.

Materials and Methods

Study approval and oversight

Experiments were performed in the University of Pittsburgh Regional Biocontainment Laboratory BSL-3 facility, which is a registered entity with the CDC/USDA for work with highly pathogenic avian influenza viruses. The study was conducted in strict accordance with the recommendations in the Guide for the Care and Use of Laboratory Animals of the National Institutes of Health. All experiments had oversight and approval by the Institutional Animal Care and Use Committee (protocol: 15055917) and the Institutional Biosafety Committee (protocol: 055-15) at the University of Pittsburgh. All personnel wore personal protective equipment and used powered air-purifying respirators (3M Versaflo) or worked in a class III biological safety cabinet.

Animals

Seven healthy adult female cynomolgus macaques (Macaca fascicularis) were confirmed to be seronegative for influenza A nucleoprotein antibodies by ELISA (Virusys) and were surgically implanted with a TA10TA-D70 telemetry device (Data Sciences International, St.

Paul, MN) placed in the abdominal wall to monitor temperature and activity as described (32). Three additional cynomolgus macaques were used as naïve controls.

H5N1 virus inoculum

Highly pathogenic avian influenza A/Vietnam/1203/2004 (H5N1) virus was kindly provided by Dr. S. Mark Tompkins at the Department of Infectious Diseases, University of Georgia. Virus propagation was carried out under BSL3 conditions at the University of Georgia. Virus stock was amplified in 10-11 day-old embryonated specific pathogen free chicken eggs (Charles River Laboratories) for 24 h as previously described (33). Allantoic fluid from inoculated eggs was clarified by centrifugation and aliquots stored at −80°C until transferred to the University of Pittsburgh Regional Biocontainment Laboratory BSL-3 facility. Virus titer was determined in Madin-Darby canine kidney cells (MDCK) by plaque assay and expressed as pfu/ml. Whole genome sequencing of virus seed and propagated stocks was performed using the Illumina MiSeq NGS platform. A comparison of the consensus sequence to publicly available A/Vietnam/1203/2004 (H5N1) sequences on the Influenza Research Database (http://www.fludb.org/) showed no amino acid changes in the virus seed and propagated stocks used in this experiment. Virus was diluted in media containing bovine serum albumin, HEPES buffer, penicillin/streptomycin and trypsin immediately prior to aerosol exposure.

Aerosol exposure

Macaques were sedated with ketamine and respiratory function including calculation of minute volume assessed by plethysmography using a head-out chamber controlled by Buxco XA software (Data Sciences International, St. Paul, MN). Macaques were then placed inside a class III biological safety cabinet (Baker) and sedation maintained by constant low-dose infusion of ketamine. The head was inserted into a head-only exposure chamber (Biaera Technologies, Hagerstown, MD). Aerosols of virus were created using an Aeroneb solo nebulizer (Aerogen, Deerfield, IL) and all aspects of exposure were controlled by the AeroMP exposure system (Biaera Technologies). Exposure duration ranged from 15 to 34 min (mean time = 24.3 min) and was determined by each macaque's minute volume, the desired presented dose, the nebulizer concentration of the virus, and the spray factor of the virus as determined by sham exposures using virus without animals as previously described (34). Aerosol samples were collected in an all-glass impinger (Ace Glass, Vineland, NJ) containing viral growth media and Antifoam A (Sigma-Aldrich, St. Louis, MO) and analyzed by plaque assay to determine the actual aerosol concentration administered. Particle size was measured using an Aerodynamic Particle Sizer (TSi, Inc., Shoreview, MN) and confirmed to be an average of 4 um in diameter.

Molecular imaging and animal sampling

Molecular imaging with 2-deoxy-2-[^{18}F]-fluoro-D-glucose (FDG) positron emission tomography (PET) and computed tomography (CT) using a micro-PE Focus 220 preclinical PET scanner (Siemens Molecular Solutions, Knoxville, TN) and an 8-slice helical CT scanner (Neurologica Corp., Danvers, MA) was done as described (35) both before infection and at day 2 post infection (PI) on all animals. Nasal saline washes and blood samples were collected pre-infection and on days 1, 2, 4 and 6 depending on survival and at the time of

necropsy. Whole blood was analyzed for absolute cell counts and processed for plasma and PBMC as described previously (36). Bronchoalveolar lavages (BAL) were performed more than two weeks pre-infection and on days 2, 4, and 6 depending on survival. Whole BAL and BAL fluid samples were aliquoted and stored at −80°C. At the time of sacrifice, animals underwent transcardiac saline perfusion and at necropsy various tissues were collected and either snap frozen in liquid nitrogen or fixed in 10% buffered formalin. Lung samples for detection of virus titers were taken from the extremities of upper, middle and lower lobes and not from deep within the tissues. Alternatively tissues were fixed in 2% paraformaldehyde for 4 h and infused with 30% sucrose overnight prior to cryopreservation as described (37).

Virus quantification

Snap frozen tissues were homogenized in media containing FBS using an Omni tissue homogenizer (Omni International). For RT-PCR, serum, BAL, or tissue homogenate was mixed with TriReagent (Ambion) and RNA extracted using either PureLink Viral RNA/DNA extraction kit (Invitrogen) or RNeasy Mini Kit (Qiagen). The SuperScript III Platinum One-Step Quantitative RT-PCR Kit (Invitrogen) was used for amplification of each RNA sample. Influenza A primers, probe, and cycling conditions used for real-time RT-PCR were followed as described in BEI Resources product information sheet NR-15592. A standard curve was generated using 10-fold dilutions of RNA from virus stock of known titer. For quantitation through plaque assay, nasal wash, BAL fluid, or homogenized tissue samples were adsorbed onto confluent monolayers of MDCK (ATCC) in duplicate wells of a 6 well plate and overlaid with agarose containing media with TPCK-trypsin. MDCK cells were newly ordered, did not contain mycoplasma, and utilized within 5 passages of thawing. Plates were incubated for 3 days at 37°C. Cells were fixed in formaldehyde, agar plugs were removed and cells were stained with crystal violet to identify plaques.

Generation of lung suspensions

Lung cell suspensions were generated as described (38) with minor modifications. Briefly, intact lung was filled via the main bronchus with Hank's balanced salt solution with Ca/Mg and HEPES buffer containing 12.9U/mL elastase and 100ug/mL DNase I without prior flushing, clamped closed, and incubated at 37°C. Lung tissue was manually disrupted and single cells were passed through a metal sieve and a 70 um cell strainer. Cells were either freshly stained with antibodies as described below or cryopreserved for later analysis.

Flow cytometric analyses

The following antibodies were used to stain blood, BAL, and lung suspension and were from BD Biosciences unless otherwise noted: CD3 (clone SP34-2) and CD20 (2H7) (combined as lineage markers), CD4 (L200), CD11b (ICRF44), CD11c (S-HCL-3), CD14 (M5E2), CD16 (3G8), CD45 (DO58-1283), CD123 (7G3), CD163 (GHI/61), CD206 (19.2), active caspase-3 (C92-605), cytokeratin (CAM5.2), Ki-67 (B56), MHC class II (L243), and influenza A virus nucleoprotein (BEI, DPJY03). The anti-nucleoprotein antibody was directly conjugated with the APEX Alexa Fluor 647 Antibody labeling kit (Thermo Fisher). Flow cytometric analysis was performed as previously described (39). Absolute counts of blood mononuclear cells, $CD4^+$ T cells, and intermediate monocytes were determined

through a quantitative flow cytometry-based assay using BD Trucount tubes (40). Cell viability in BAL and lung suspensions was analyzed immediately after processing through trypan blue staining and determined to be greater than 98% in each preparation. Between 1-2×10^6 cells were stained within 30 min of completing sample processing and were maintained on ice for the entirety of the stain. Matched isotype control antibodies were utilized to define specific staining above autofluorescence. Where appropriate, cellular debris was excluded by use of FSC-A and SSC-A gating. All samples were run on a BD FACS Aria using BD FACS Diva software in the Regional Biocontainment Laboratory and analysis was performed using Flowjo software version 9.7.7 (Treestar).

Analysis of cytokine and albumin concentrations

A 13-plex nonhuman primate specific cytokine/chemokine LEGENDplex bead array (BioLegend) was used according to the manufacturer protocol on plasma and BAL fluid samples. All samples were run on a BD FACS Aria and analysis was performed using LEGENDplex analysis software (Biolegend). An ELISA specific for cynomolgus/rhesus IFN-α2 was performed using BAL samples according to manufacturer protocol (PBL, VeriKine). BAL fluids from post-infection time points were diluted 50-fold in order to remain within the standard limits of detection. An anti-monkey albumin ELISA was used to quantify albumin concentrations in the BAL fluid and plasma (Innovative Research). Plasma was diluted according to the manufacturer protocol and BAL fluid was diluted either 1,000-fold for pre-infection samples or 20,000-fold for post-infection samples.

In situ hybridization and immunofluorescence

In situ hybridization of formalin-fixed tissues was performed using ^{35}S-labeled riboprobes synthesized using templates derived from 760 base pairs of influenza A/California/04/2009 matrix protein as previously described (41). For immunohistochemistry, sections were blocked in 5% serum prior to adding primary antibody for 1.5h at 4°C. The following antibodies were used: mouse anti-pan cytokeratin (AE1/AE3, Abcam), mouse anti-human IFN-α (MMHA-2, PBL Interferon Source), rabbit anti-human IFN-α2 (Thermo Scientific), mouse anti-human calprotectin Ab-1 (MAC 387, Thermo Scientific), mouse anti-human MCP-1 (5D3-F7, BioLegend), mouse anti-human MCP-1 biotin (5D3-F7, BioLegend), mouse anti-human CD163 biotin (eBioGHI/61, eBioscience), anti-influenza A nucleoprotein (DPJY03, BEI Resources), and mouse anti-human CD206 (15-2, AbD Serotec). Secondary antibodies were from Thermo Fischer Scientific and included goat anti-mouse IgG1 Alexa Fluor 546, goat anti-mouse IgG2a Alexa Fluor 647, donkey anti-rabbit IgG Alexa Fluor 488, and donkey anti-rabbit IgG Alexa Fluor 546. Biotinylated antibodies were detected using the HRP-Streptavidin and Alexa Fluor 488 Tyramide Signal Amplification kit. Cell nuclei were identified using membrane permeable Hoescht dye and slides were mounted in Gelvatol mounting media and viewed on an Olympus Fluoview 1000 confocal microscope. All staining included an appropriately concentrated isotype-matched control antibody.

Statistics

All statistical analyses were performed in Prism v6.0 (GraphPad). The p values less than 0.05 are considered significant. All analyses were performed using two-tailed, non-parametric tests, either between control and infected animals or between paired samples.

Significant *p* values from one-way ANOVA tests were followed up by Dunn's multiple comparison tests. A Grubbs' test was used to determine whether any data points were considered to be significant outliers. The averages of $\log_{10}$ values were calculated as geometric means.

Results

Aerosolized H5N1 infection of macaques causes fulminant pneumonia

We exposed 7 adult cynomolgus macaques that were seronegative to influenza A viruses to small-particle aerosols of highly pathogenic avian influenza A/Vietnam/1203/2004 (H5N1), a well-defined strain isolated from a fatal human case that is commonly used in this macaque species (21–23, 26). Sedated macaques in a head-only chamber within a class III biological safety cabinet were exposed to aerosols averaging 4 um in diameter that were generated using an electronic vibrating nebulizer. The mean challenge dose was 6.72 $\log_{10}$ plaque forming units (pfu) (Table I), which is similar to the amount given by intratracheal inoculation in previous reports using this strain (21–23, 26). All animals had a fever that peaked within 24 h of infection as determined by radiotelemetry (Fig 1A). Infection had almost immediate effects on respiratory function as determined by plethysmography, with increases in respiration rate and decreases in tidal volume and expiratory time by 1-2 days PI, consistent with acute lower respiratory tract disease (Fig 1B). To visualize the effects of infection on the lung we did molecular imaging, combining PET using the radiotracer FDG to label metabolically-active cells with CT to define anatomy. Imaging at day 2 PI revealed severe, diffuse inflammation in the lungs of all animals, with significant increases in FDG uptake and lung volume relative to pre-infection time points (Fig 1, C and D). These findings are consistent with the acute respiratory distress syndrome that characterizes progressive human H5N1 infection (1).

Aerosolized infection is associated with systemic H5N1 virus replication

Respiratory disease rapidly progressed in all animals, with 3 animals dying and 4 animals being humanely sacrificed between 2 and 6 days PI (mean = 3.2 days) with respiratory failure (Table I). At necropsy lungs were intensely hemorrhagic, exhibited intra-alveolar exudate and cellular consolidation, and were grossly enlarged, increasing 3- to 4-fold in weight relative to body weight-matched uninfected controls (Fig 2A–C). The increased mass of lung was attributed to fluid accumulation as cell yield following enzymatic lung digestion was not different between infected and uninfected macaques (Fig 2D). Infectious virus was intermittently recovered at relatively low titer in nasal washes but was consistently isolated from BAL fluid and was present at high titer in all regions of both lungs at necropsy (Table I). Semi-quantitative real-time RT-PCR showed uniform and remarkably consistent titers of H5N1 virus in the extremities of upper, middle and lower regions of both lungs in all animals and revealed significant virus replication in other tissues, most notably lung-draining hilar lymph nodes (Fig 2E). Virus replication was confirmed by in situ hybridization against H5N1 matrix RNA, which showed intense replication in cells lining most alveoli. Viral RNA was readily detected by in situ hybridization in hilar lymph nodes and duodenum lamina propria, confirming systemic infection (Fig 2F).

Profound inflammatory response to H5N1 infection in blood and airways of macaques

To begin to define the mechanisms driving lethal disease following aerosol H5N1 inoculation we first analyzed the cellular response to infection in blood and BAL. Infection produced profound leukopenia at day 1 and 2 PI with loss of $CD45^+$ mononuclear cells and depletion of $CD4^+$ T lymphocytes (Fig 3, A and B), consistent with findings in H5N1 infected humans (12, 42). In contrast, there was a significant increase in the number of $CD14^+CD16^+$ intermediate monocytes in blood (Fig 3, A and B). The cellularity of BAL did not change with infection (Fig 3C) but the constituent cell populations were dramatically altered. Alveolar macrophages are the predominant cell recovered from BAL in health, and in the macaque alveolar macrophages are defined as being $CD163^+CD206^+$, distinguishing them from $CD163^+CD206^-$ interstitial macrophages (43). Due to autofluorescence of cells in BAL fluid, matched isotype controls were utilized with every experiment to ensure macrophage populations were clearly defined (Supplementary Fig 1A). Up to 50% of all cells in BAL prior to infection were $CD163^+CD206^+$ alveolar macrophages, which were decimated within 2 days of aerosol exposure, coincident with an influx of MHC, class II^-CD11b^+ neutrophils. As expected $CD163^+CD206^-$ interstitial macrophages made up an insignificant percentage of cells in BAL before infection, but there was evidence in some animals that infection resulted in a modest increase in interstitial macrophages recovered from BAL (Fig 3, D and E). Given that hypercytokinemia is a prominent characteristic of fatal human H5N1 infection (12) we measured a panel of proinflammatory cytokines and chemokines in plasma and BAL using a cytokine bead array before and after infection. There was a transient but profound increase in several proinflammatory factors in plasma, including IL-6, eotaxin, IP-10, and MCP-1, with plasma IL-6 in particular increasing over 500-fold within 1 day of infection and then declining (Fig 3F). There was a massive increase in the concentration of proinflammatory cytokines and chemokines in BAL measured at day 2 PI, with 12 out of 13 analytes significantly increasing. Many proinflammatory cytokines and chemokines in BAL increased several hundred times, with IL-6 increasing 1,000-fold (Fig 3G). Notably, the antiviral protein interferon (IFN)-α increased 2,000-fold in BAL following H5N1 infection, reaching concentrations of 10 to 100 ng/ml at 2 days PI (Fig 3H).

Reciprocal effects of H5N1 infection on alveolar and interstitial macrophages in lung

We next assessed the cellular response to H5N1 infection in lung cell suspensions, which were enzymatically digested without prior flushing of airways and thus contained both airway and interstitial cells. As with cells in BAL, matched isotype control antibodies were used with each stain to ensure cell populations were appropriately identified (Supplementary Fig 1B and C). The number of AEC, identified by expression of cytokeratin 7/8 (44), recovered from lungs was dramatically decreased as a result of infection in 4 out 5 animals, but due to an outlier this effect was not significant (Fig 4, A and B). Alveolar macrophages were massively depleted from lung following infection, consistent with findings in BAL, whereas the number of interstitial macrophages, differentiated from the alveolar subset by lack of CD206 expression, increased four-fold. $Lineage^-$MHC class $II^+CD206^-CD123^+$ plasmacytoid dendritic cells (DC) constituted a minor population of cells in uninfected lung, which was significantly reduced following infection, whereas the proportion of $Lineage^-$MHC class II^+ $CD206^-CD11c^+$ myeloid DC was unchanged (Fig 4, A and B). Interstitial macrophages had significant increases in expression of Ki-67 following infection,

revealing recent cell division, whereas the long-lived alveolar macrophages showed no evidence of recent division (Fig 4, C and D).

We used immunofluorescence of lung sections to validate and extend flow cytometry findings. Preliminary experiments showed that $CD206^+$ alveolar macrophages all co-expressed CD163, whereas CD163+ macrophages in the lung parenchyma lacked expression of CD206, consistent with flow cytometry data. We therefore for simplicity used antibodies to CD206 and CD163 to identify alveolar and interstitial macrophages, respectively, in lung sections. $CD206^+$ alveolar macrophages were readily identified prior to infection but were only rarely present after infection, consistent with findings in BAL and lung suspensions. Conversely, there was a massive influx of $CD163^+$ interstitial macrophages following infection (Fig 4E). Neutrophils, identified by expression of calprotectin (45), were massively increased in lung sections following infection (Fig 4E). Immunofluorescence revealed that AEC and to a greater extent neutrophils produced IFN-α following infection, and MCP-1 expression was seen by both cell types. In contrast, infiltrating interstitial macrophages were not found to express IFN-α or MCP-1 (Fig 4F).

Extensive infection of alveolar macrophages and AEC with loss of epithelial barrier function

We used immunofluorescence to identify the specific cellular targets of H5N1 in the lung using antibody to viral nucleoprotein to identify replicating virus. Nucleoprotein staining substantially co-localized with cytokeratin in alveoli, indicating widespread infection of AEC. Both the highly flattened type I pneumocytes and cuboidal type II pneumocytes extensively expressed virus nucleoprotein (Fig 5A). Virus replication was detected in alveolar macrophages, although these cells were more difficult to identify because of massive depletion. In contrast, no nucleoprotein staining could be detected in the vast number of infiltrating interstitial macrophages present in infected lung (Fig 5A). Flow cytometric analysis of lung cell suspensions revealed that approximately 20% of all AEC and alveolar macrophages were infected with H5N1, approaching more than 30% in some animals. Infection of interstitial macrophages averaged less than 5% across animals (Fig 5, B and C). Infection of AEC lead to their apoptosis, as active caspase-3 expression was significantly greater in nucleoprotein-expressing AEC as compared to uninfected AEC in lung cell suspensions from the same animal (Fig 5D). To determine if AEC death could have contributed to the leakage of fluid into the alveolar airspace that resulted in acute respiratory distress syndrome following infection, we measured the concentration in BAL of albumin, a large plasma protein that is normally excluded from the airway by an intact epithelial barrier. The concentration of albumin in BAL increased 20-fold in macaques at day 2 PI, and in the 3 animals surviving to day 4–6 PI albumin concentration in BAL was 90 times greater than pre-infection levels. This was not a function of hemoconcentration in severely ill animals as albumin concentrations in plasma did not significantly change with infection (Fig 5E).

Discussion

Our study reveals for the first time that inhalation of small particle aerosols of highly pathogenic avian influenza A (H5N1) virus in cynomolgus macaques induces bilateral

pneumonia that rapidly progresses to the acute respiratory distress syndrome and death, recapitulating human disease. All previous nonhuman primate studies using newly emerged H5N1 viruses beginning in 2001 have exposed macaques to virus using liquid suspensions instilled into the trachea, often combined with inoculation into the nose, mouth and eye, an approach that rarely has produced fatal disease (21–26). Studies from three independent groups using the same A/Vietnam/1203/2004 (H5N1) isolate at a similar challenge dose (mean = 7.05 $\log_{10}$ pfu) and in the same species of macaque as used here reported fatality in just 2/24 (8.3%) animals (21–23, 26).

Avian influenza viruses prefer binding to sialic acid linked to galactose via an α-2,3 linkage, and these receptors predominate in the human and nonhuman primate lower respiratory tract rather than the trachea and upper respiratory tract (5, 8). While H5N1 virus isolates can infect *ex vivo* cultures of human nasopharyngeal, adenoid and tonsillar tissues (4) our finding that infectious virus was only intermittently recovered from nasal washes at low titers relative to BAL fluid, despite passage of inhaled virus through the nasopharynx, suggests that the upper respiratory tract is not a major site of replication *in vivo*. H5N1 infection in macaques was systemic based on high titer of virus in hilar lymph nodes and recovery from peripheral lymph nodes and gastrointestinal tract, although it is possible that the gut was seeded independently through swallowing of virus during aerosol exposure. In human H5N1 cases diarrheal disease is a common presentation and is associated with recovery of virus from feces, consistent with virus replication in the gastrointestinal tract (46).

Close contact with infected domestic poultry is the predominant risk factor for acquiring H5N1 influenza virus infection in humans (47), however the precise means of avian-to-human transmission remains unknown. Our data indicate that aerosol exposure may be an important source of human H5N1 infections. Sneezing and coughing in H5N1-infected poultry are reported infrequently as affected animals are typically found comatose or dead with few clinical signs (48). This suggests that respiratory-derived aerosols are an uncommon source of H5N1 virus from infected birds, in contrast to human-to-human transmission of seasonal influenza viruses (49, 50). This may account for the rarity of human infections despite widespread exposure to infected poultry in affected countries (51, 52). H5N1 virus can be recovered from feces and skin of infected birds (48, 53), and manure and skin contribute significantly to fine dust particles (< 4 um diameter) commonly found inside and outside of poultry houses (54), although virus infectivity is rapidly lost in feces upon drying (53). Of greater potential for airborne transmission is inadvertent generation of small-particle aerosols of virus during defeathering and preparing sick or dead poultry for consumption, and this practice is one of the greatest risk factors for human H5N1 infection (47).

Our findings reveal that direct virus-mediated damage to alveoli is a key factor in driving disease severity. Inhalation of aerosolized H5N1 virus resulted in massive infection and apoptosis of AEC, consistent with findings in patients (6) and *in vitro* (10). Both type I pneumocytes that facilitate gas exchange and type II pneumocytes that secrete surfactant and serve as progenitors for both pneumocyte subsets were affected, accounting for the extreme compromise in respiratory function. Notably, AEC infection was associated with marked

protein leakage into the alveolar space reflecting loss of epithelial barrier function that is a hallmark of the acute respiratory distress syndrome (55). AEC were also found to produce MCP-1, one of the proinflammatory factors that was substantially increased in plasma and BAL fluid and which is correlated with fatal H5N1 infection in humans (12). Indeed, the intense production of proinflammatory cytokines in airways, with 500-1,000 fold increases in IL-6, eotaxin, IP-10 and IL-8 at 2 days of infection, could reflect the extensive infection of AEC following aerosol infection with H5N1. By comparison, intratracheal infection of macaques with the 1918 influenza virus was associated with modest 25-fold increases in plasma IL-6 by 8 days PI (56).

Inhalation of airborne H5N1 virus also led to up to 30% of alveolar macrophages being infected, resulting in rapid decimation of these cells. Loss of alveolar macrophages would contribute directly to disease through loss of regulatory function (11), and experimental depletion of alveolar macrophages in sublethal influenza virus infection of mice and pigs exacerbates pulmonary inflammation, edema and fluid leakage (57–59). Loss of alveolar macrophages was offset by massive infiltration of interstitial macrophages, although the function of these newly recruited macrophages remains unclear. Infiltrating interstitial macrophages had recently divided, as distinct from the alveolar macrophages, indicating they were not simply alveolar macrophages that had down-regulated CD206 expression. Macrophage infiltration was associated with significant increases in intermediate $CD14^{+}CD16^{+}$ monocytes that have an inflammatory function (60) and were likely recruited to lung via increased MCP-1 (61). Infiltrating macrophages contribute to AEC apoptosis in murine influenza models (62, 63) but in our study AEC apoptosis was primarily a consequence of AEC infection. Macrophages and TNF/iNOS producing DC have been implicated in cytokine production and immunopathology in murine models (64, 65). A hallmark of these cells in murine influenza is high level production of TNF-α (65), but recently recruited interstitial macrophages in macaques in our study produced negligible amounts of TNF-α by intracellular cytokine staining (data not shown), and TNF-α was one of the least significant cytokines present in BAL fluid after infection. It is possible that interstitial macrophages are recruited in part to repopulate decimated alveolar macrophages, as has been demonstrated in other macaque models (43). The marginal increase in $CD163^{+}CD206^{-}$ macrophages in BAL at day 2 PI would suggest this was not a significant effect, although the rapidity of disease could be a factor in limiting transmigration of macrophages into airways.

A notable feature of H5N1 infection in our study was the profound production of IFN-α in the distal airways, which increased nearly 2,000-fold by 2 days PI in all animals. IFN-α was produced to a modest extent by AEC but was primarily found in infiltrating neutrophils in animals at necropsy. The principal source of type I IFN in pulmonary infection with RNA viruses is the alveolar macrophage (66), and it is possible that in the early stages of infection prior to their decimation alveolar macrophages accounted for this massive production of IFN-α in airways. Influenza A/Vietnam/1203/2004 (H5N1) infection induces strong induction of type I and III IFN in human cell lines *in vitro* but results in a paradoxical downregulation of IFN-stimulated genes relative to the less pathogenic 2009 pandemic H1N1 influenza virus, an effect that is linked to H5N1 virus NS1 (67). Similarly, in macaques infected with an identical H5N1 isolate type I IFN gene expression in lung was

robust early in infection but IFN-stimulated gene expression was limited relative to infection with less pathogenic H5N1 isolates, associated with a failure to suppress virus replication (23). These data suggest that H5N1 virus antagonizes IFN-stimulated gene expression despite intense IFN-α induction, facilitating massive virus replication that leads to alveolar destruction.

A limitation of our study is that only one virus strain given at a relatively high challenge dose was used in all animals. It will be important both in terms of public health significance and therapeutic intervention to determine the susceptibility of macaques to a range of doses of aerosolized H5N1 virus and to identify the point at which disease severity is attenuated and survival prolonged. Similarly, comparative studies with a less pathogenic strain that disseminates throughout the lower respiratory tract following aerosolization would allow us to definitively address the mechanism for mortality following H5N1 infection. A good candidate for such studies is 2009 pandemic H1N1, which replicates in lungs and other organs of macaques (68) but does not induce significant disease when delivered by small-particle aerosol (69).

Our data support the notion that rapid initiation of therapies targeting virus replication is indicated in the treatment of H5N1 pneumonia, as opposed to therapies targeting cytokines, consistent with recent murine studies (20). The work establishes aerosolized H5N1 infection of nonhuman primates as the model of choice for evaluating potential antiviral therapies in the treatment of highly pathogenic avian influenza virus infection of humans, as well as testing promising H5N1 vaccine approaches for their ability to prevent fulminant lower respiratory tract disease.

Supplementary Material

Refer to Web version on PubMed Central for supplementary material.

Acknowledgments

The authors wish to thank Dana Gillis and Nicole McKinney for veterinary assistance and Michael Kujawa, Aaron Walters, Guoji Wang, Mark Stauffer and Dana Weber for technical assistance.

Abbreviations

BAL	bronchoalveolar lavage
AM	alveolar macrophage
IM	interstitial macrophage
AEC	alveolar epithelial cells
PET	positron emission tomography
FDG	2-deoxy-2-[^{18}F]-fluoro-D-glucose
CT	computed tomography

pDC	plasmacytoid dendritic cell
mDC	myeloid dendritic cell
Gr	granulocytes
MDCK	Madin-Darby canine kidney

References

1. Writing Committee of the Second World Health Organization Consultation on Clinical Aspects of Human Infection with Avian Influenza. Abdel-Ghafar AN, Chotpitayasunondh T, Gao Z, Hayden FG, Nguyen DH, de Jong MD, Naghdaliyev A, Peiris JS, Shindo N, Soeroso S, Uyeki TM. Update on avian influenza A (H5N1) virus infection in humans. N Engl J Med. 2008; 358:261–273. [PubMed: 18199865]
2. Jhung MA, Nelson DI, C. Centers for Disease, and Prevention. Outbreaks of avian influenza A (H5N2), (H5N8), and (H5N1) among birds–United States, December 2014-January 2015. MMWR Morb Mortal Wkly Rep. 2015; 64:111. [PubMed: 25654614]
3. Arriola CS, Nelson DI, Deliberto TJ, Blanton L, Kniss K, Levine MZ, Trock SC, Finelli L, Jhung MA, H5 Investigation Group. Infection risk for persons exposed to highly pathogenic avian influenza A H5 virus-Infected birds, United States, December 2014-March 2015. Emerg Infect Dis. 2015; 21:2135–2140. [PubMed: 26583382]
4. Nicholls JM, Chan MC, Chan WY, Wong HK, Cheung CY, Kwong DL, Wong MP, Chui WH, Poon LL, Tsao SW, Guan Y, Peiris JS. Tropism of avian influenza A (H5N1) in the upper and lower respiratory tract. Nat Med. 2007; 13:147–149. [PubMed: 17206149]
5. Shinya K, Ebina M, Yamada S, Ono M, Kasai N, Kawaoka Y. Avian flu: influenza virus receptors in the human airway. Nature. 2006; 440:435–436. [PubMed: 16554799]
6. Uiprasertkul M, Kitphati R, Puthavathana P, Kriwong R, Kongchanagul A, Ungchusak K, Angkasekwinai S, Chokephaibulkit K, Srisook K, Vanprapar N, Auewarakul P. Apoptosis and pathogenesis of avian influenza A (H5N1) virus in humans. Emerg Infect Dis. 2007; 13:708–712. [PubMed: 17553248]
7. Uiprasertkul M, Puthavathana P, Sangsiriwut K, Pooruk P, Srisook K, Peiris M, Nicholls JM, Chokephaibulkit K, Vanprapar N, Auewarakul P. Influenza A H5N1 replication sites in humans. Emerg Infect Dis. 2005; 11:1036–1041. [PubMed: 16022777]
8. van Riel D, Munster VJ, de Wit E, Rimmelzwaan GF, Fouchier RA, Osterhaus AD, Kuiken T. H5N1 virus attachment to lower respiratory tract. Science. 2006; 312:399. [PubMed: 16556800]
9. Gu J, Xie Z, Gao Z, Liu J, Korteweg C, Ye J, Lau LT, Lu J, Gao Z, Zhang B, McNutt MA, Lu M, Anderson VM, Gong E, Yu AC, Lipkin WI. H5N1 infection of the respiratory tract and beyond: a molecular pathology study. Lancet. 2007; 370:1137–1145. [PubMed: 17905166]
10. Daidoji T, Koma T, Du A, Yang CS, Ueda M, Ikuta K, Nakaya T. H5N1 avian influenza virus induces apoptotic cell death in mammalian airway epithelial cells. J Virol. 2008; 82:11294–11307. [PubMed: 18787012]
11. Holt PG. Down-regulation of immune responses in the lower respiratory tract: the role of alveolar macrophages. Clin Exp Immunol. 1986; 63:261–270. [PubMed: 3516464]
12. de Jong MD, Simmons CP, Thanh TT, Hien VM, Smith GJ, Chau TN, Hoang DM, Chau NV, Khanh TH, Dong VC, Qui PT, Cam BV, Ha do Q, Guan Y, Peiris JS, Chinh NT, Hien TT, Farrar J. Fatal outcome of human influenza A (H5N1) is associated with high viral load and hypercytokinemia. Nat Med. 2006; 12:1203–1207. [PubMed: 16964257]
13. Guan Y, Poon LL, Cheung CY, Ellis TM, Lim W, Lipatov AS, Chan KH, Sturm-Ramirez KM, Cheung CL, Leung YH, Yuen KY, Webster RG, Peiris JS. H5N1 influenza: a protean pandemic threat. Proc Natl Acad Sci U S A. 2004; 101:8156–8161. [PubMed: 15148370]
14. Peiris JS, Yu WC, Leung CW, Cheung CY, Ng WF, Nicholls JM, Ng TK, Chan KH, Lai ST, Lim WL, Yuen KY, Guan Y. Re-emergence of fatal human influenza A subtype H5N1 disease. Lancet. 2004; 363:617–619. [PubMed: 14987888]

15. To KF, Chan PK, Chan KF, Lee WK, Lam WY, Wong KF, Tang NL, Tsang DN, Sung RY, Buckley TA, Tam JS, Cheng AF. Pathology of fatal human infection associated with avian influenza A H5N1 virus. J Med Virol. 2001; 63:242–246. [PubMed: 11170064]
16. Chan MC, Cheung CY, Chui WH, Tsao SW, Nicholls JM, Chan YO, Chan RW, Long HT, Poon LL, Guan Y, Peiris JS. Proinflammatory cytokine responses induced by influenza A (H5N1) viruses in primary human alveolar and bronchial epithelial cells. Respir Res. 2005; 6:135. [PubMed: 16283933]
17. Cheung CY, Poon LL, Lau AS, Luk W, Lau YL, Shortridge KF, Gordon S, Guan Y, Peiris JS. Induction of proinflammatory cytokines in human macrophages by influenza A (H5N1) viruses: a mechanism for the unusual severity of human disease? Lancet. 2002; 360:1831–1837. [PubMed: 12480361]
18. Lee SM, Gardy JL, Cheung CY, Cheung TK, Hui KP, Ip NY, Guan Y, Hancock RE, Peiris JS. Systems-level comparison of host-responses elicited by avian H5N1 and seasonal H1N1 influenza viruses in primary human macrophages. PloS one. 2009; 4:e8072. [PubMed: 20011590]
19. Peiris JS, Cheung CY, Leung CY, Nicholls JM. Innate immune responses to influenza A H5N1: friend or foe? Trends Immunol. 2009; 30:574–584. [PubMed: 19864182]
20. Salomon R, Hoffmann E, Webster RG. Inhibition of the cytokine response does not protect against lethal H5N1 influenza infection. Proc Natl Acad Sci U S A. 2007; 104:12479–12481. [PubMed: 17640882]
21. Baskin CR, Bielefeldt-Ohmann H, Tumpey TM, Sabourin PJ, Long JP, Garcia-Sastre A, Tolnay AE, Albrecht R, Pyles JA, Olson PH, Aicher LD, Rosenzweig ER, Murali-Krishna K, Clark EA, Kotur MS, Fornek JL, Proll S, Palermo RE, Sabourin CL, Katze MG. Early and sustained innate immune response defines pathology and death in nonhuman primates infected by highly pathogenic influenza virus. Proc Natl Acad Sci U S A. 2009; 106:3455–3460. [PubMed: 19218453]
22. Cilloniz C, Shinya K, Peng X, Korth MJ, Proll SC, Aicher LD, Carter VS, Chang JH, Kobasa D, Feldmann F, Strong JE, Feldmann H, Kawaoka Y, Katze MG. Lethal influenza virus infection in macaques is associated with early dysregulation of inflammatory related genes. PLoS Pathog. 2009; 5:e1000604. [PubMed: 19798428]
23. Muramoto Y, Shoemaker JE, Le MQ, Itoh Y, Tamura D, Sakai-Tagawa Y, Imai H, Uraki R, Takano R, Kawakami E, Ito M, Okamoto K, Ishigaki H, Mimuro H, Sasakawa C, Matsuoka Y, Noda T, Fukuyama S, Ogasawara K, Kitano H, Kawaoka Y. Disease severity is associated with differential gene expression at the early and late phases of infection in nonhuman primates infected with different H5N1 highly pathogenic avian influenza viruses. J Virol. 2014; 88:8981–8997. [PubMed: 24899188]
24. Rimmelzwaan GF, Kuiken T, van Amerongen G, Bestebroer TM, Fouchier RA, Osterhaus AD. Pathogenesis of influenza A (H5N1) virus infection in a primate model. J Virol. 2001; 75:6687–6691. [PubMed: 11413336]
25. Shinya K, Gao Y, Cilloniz C, Suzuki Y, Fujie M, Deng G, Zhu Q, Fan S, Makino A, Muramoto Y, Fukuyama S, Tamura D, Noda T, Eisfeld AJ, Katze MG, Chen H, Kawaoka Y. Integrated clinical, pathologic, virologic, and transcriptomic analysis of H5N1 influenza virus-induced viral pneumonia in the rhesus macaque. J Virol. 2012; 86:6055–6066. [PubMed: 22491448]
26. Soloff AC, Bissel SJ, Junecko BF, Giles BM, Reinhart TA, Ross TM, Barratt-Boyes SM. Massive mobilization of dendritic cells during influenza A virus subtype H5N1 infection of nonhuman primates. J Infect Dis. 2014; 209:2012–2016. [PubMed: 24403559]
27. Fujiyuki T, Yoneda M, Yasui F, Kuraishi T, Hattori S, Kwon HJ, Munekata K, Kiso Y, Kida H, Kohara M, Kai C. Experimental infection of macaques with a wild water bird-derived highly pathogenic avian influenza virus (H5N1). PloS one. 2013; 8:e83551. [PubMed: 24367600]
28. Knight V. Viruses as agents of airborne contagion. Ann N Y Acad Sci. 1980; 353:147–156. [PubMed: 6261640]
29. Tellier R. Review of aerosol transmission of influenza A virus. Emerg Infect Dis. 2006; 12:1657–1662. [PubMed: 17283614]
30. Gustin KM, Belser JA, Wadford DA, Pearce MB, Katz JM, Tumpey TM, Maines TR. Influenza virus aerosol exposure and analytical system for ferrets. Proc Natl Acad Sci U S A. 2011; 108:8432–8437. [PubMed: 21536880]

31. Lednicky JA, Hamilton SB, Tuttle RS, Sosna WA, Daniels DE, Swayne DE. Ferrets develop fatal influenza after inhaling small particle aerosols of highly pathogenic avian influenza virus A/Vietnam/1203/2004 (H5N1). Virol J. 2010; 7:231. [PubMed: 20843329]

32. Hartman AL, Powell DS, Bethel LM, Caroline AL, Schmid RJ, Oury T, Reed DS. Aerosolized rift valley fever virus causes fatal encephalitis in african green monkeys and common marmosets. J Virol. 2014; 88:2235–2245. [PubMed: 24335307]

33. Song H, Nieto GR, Perez DR. A new generation of modified live-attenuated avian influenza viruses using a two-strategy combination as potential vaccine candidates. J Virol. 2007; 81:9238–9248. [PubMed: 17596317]

34. Hartings JM, Roy CJ. The automated bioaerosol exposure system: preclinical platform development and a respiratory dosimetry application with nonhuman primates. J Pharmacol Toxicol Methods. 2004; 49:39–55. [PubMed: 14670693]

35. Lin PL, Coleman T, Carney JP, Lopresti BJ, Tomko J, Fillmore D, Dartois V, Scanga C, Frye LJ, Janssen C, Klein E, Barry CE 3rd, Flynn JL. Radiologic responses in cynomolgous macaques for assessing tuberculosis chemotherapy regimens. Antimicrob Agents Chemother. 2013; 57:4237–4244. [PubMed: 23796926]

36. Brown KN, Trichel A, Barratt-Boyes SM. Parallel loss of myeloid and plasmacytoid dendritic cells from blood and lymphoid tissue in simian AIDS. J Immunol. 2007; 178:6958–6967. [PubMed: 17513745]

37. Swan ZD, Wonderlich ER, Barratt-Boyes SM. Macrophage accumulation in gut mucosa differentiates AIDS from chronic SIV infection in rhesus macaques. Eur J Immunol. 2016; 46:446–454. [PubMed: 26549608]

38. Wang J, Oberley-Deegan R, Wang S, Nikrad M, Funk CJ, Hartshorn KL, Mason RJ. Differentiated human alveolar type II cells secrete antiviral IL-29 (IFN-lambda 1) in response to influenza A infection. J Immunol. 2009; 182:1296–1304. [PubMed: 19155475]

39. Brown KN, Wijewardana V, Liu X, Barratt-Boyes SM. Rapid influx and death of plasmacytoid dendritic cells in lymph nodes mediate depletion in acute simian immunodeficiency virus infection. PLoS Pathog. 2009; 5:e1000413. [PubMed: 19424421]

40. Brown KN, Barratt-Boyes SM. Surface phenotype and rapid quantification of blood dendritic cell subsets in the rhesus macaque. J Med Primatol. 2009; 38:272–278. [PubMed: 19344375]

41. Bissel SJ, Giles BM, Wang G, Olevian DC, Ross TM, Wiley CA. Acute murine H5N1 influenza A encephalitis. Brain Pathol. 2012; 22:150–158. [PubMed: 21714828]

42. Tran TH, Nguyen TL, Nguyen TD, Luong TS, Pham PM, Nguyen v V, Pham TS, Vo CD, Le TQ, Ngo TT, Dao BK, Le PP, Nguyen TT, Hoang TL, Cao VT, Le TG, Nguyen DT, Le HN, Nguyen KT, Le HS, Le VT, Christiane D, Tran TT, Menno de J, Schultsz C, Cheng P, Lim W, Horby P, Farrar J, World Health Organization International Avian Influenza Investigative Team. Avian influenza A (H5N1) in 10 patients in Vietnam. N Engl J Med. 2004; 350:1179–1188. [PubMed: 14985470]

43. Cai Y, Sugimoto C, Arainga M, Alvarez X, Didier ES, Kuroda MJ. In vivo characterization of alveolar and interstitial lung macrophages in rhesus macaques: implications for understanding lung disease in humans. J Immunol. 2014; 192:2821–2829. [PubMed: 24534529]

44. Wang J, Edeen K, Manzer R, Chang Y, Wang S, Chen X, Funk CJ, Cosgrove GP, Fang X, Mason RJ. Differentiated human alveolar epithelial cells and reversibility of their phenotype in vitro. Am J Respir Cell Mol Biol. 2007; 36:661–668. [PubMed: 17255555]

45. Mattila JT, Ojo OO, Kepka-Lenhart D, Marino S, Kim JH, Eum SY, Via LE, Barry CE 3rd, Klein E, Kirschner DE, Morris SM Jr, Lin PL, Flynn JL. Microenvironments in tuberculous granulomas are delineated by distinct populations of macrophage subsets and expression of nitric oxide synthase and arginase isoforms. J Immunol. 2013; 191:773–784. [PubMed: 23749634]

46. de Jong MD, Bach VC, Phan TQ, Vo MH, Tran TT, Nguyen BH, Beld M, Le TP, Truong HK, Nguyen VV, Tran TH, Do QH, Farrar J. Fatal avian influenza A (H5N1) in a child presenting with diarrhea followed by coma. N Engl J Med. 2005; 352:686–691. [PubMed: 15716562]

47. Dinh PN, Long HT, Tien NT, Hien NT, Mai le TQ, Phong le H, Tuan le V, Van Tan H, Nguyen NB, Van Tu P, Phuong NT, World Health Organization/Global Outbreak Alert Response Network

Avian Influenza Investigation Team in Vietnam. Risk factors for human infection with avian influenza A H5N1, Vietnam, 2004. Emerg Infect Dis. 2006; 12:1841–1847. [PubMed: 17326934]

48. Swayne DE, Suarez DL. Highly pathogenic avian influenza. Rev Sci Tech. 2000; 19:463–482. [PubMed: 10935274]
49. Lindsley WG, Blachere FM, Thewlis RE, Vishnu A, Davis KA, Cao G, Palmer JE, Clark KE, Fisher MA, Khakoo R, Beezhold DH. Measurements of airborne influenza virus in aerosol particles from human coughs. PloS one. 2010; 5:e15100. [PubMed: 21152051]
50. Lindsley WG, Noti JD, Blachere FM, Thewlis RE, Martin SB, Othumpangat S, Noorbakhsh B, Goldsmith WT, Vishnu A, Palmer JE, Clark KE, Beezhold DH. Viable influenza A virus in airborne particles from human coughs. J Occup Environ Hyg. 2015; 12:107–113. [PubMed: 25523206]
51. Fielding R, Bich TH, Quang LN, Lam WW, Leung GM, Tien TQ, Ho EY, Anht le V. Live poultry exposures, Hong Kong and Hanoi, 2006. Emerg Infect Dis. 2007; 13:1065–1067. [PubMed: 18214181]
52. Vong S, Coghlan B, Mardy S, Holl D, Seng H, Ly S, Miller MJ, Buchy P, Froehlich Y, Dufourcq JB, Uyeki TM, Lim W, Sok T. Low frequency of poultry-to-human H5NI virus transmission, southern Cambodia, 2005. Emerg Infect Dis. 2006; 12:1542–1547. [PubMed: 17176569]
53. Shortridge KF, Zhou NN, Guan Y, Gao P, Ito T, Kawaoka Y, Kodihalli S, Krauss S, Markwell D, Murti KG, Norwood M, Senne D, Sims L, Takada A, Webster RG. Characterization of avian H5N1 influenza viruses from poultry in Hong Kong. Virology. 1998; 252:331–342. [PubMed: 9878612]
54. Lai HT, Nieuwland MG, Aarnink AJ, Kemp B, Parmentier HK. Effects of 2 size classes of intratracheally administered airborne dust particles on primary and secondary specific antibody responses and body weight gain of broilers: a pilot study on the effects of naturally occurring dust. Poult Sci. 2012; 91:604–615. [PubMed: 22334735]
55. Short KR, Kroeze EJ, Fouchier RA, Kuiken T. Pathogenesis of influenza-induced acute respiratory distress syndrome. Lancet Infect Dis. 2014; 14:57–69. [PubMed: 24239327]
56. Kobasa D, Jones SM, Shinya K, Kash JC, Copps J, Ebihara H, Hatta Y, Kim JH, Halfmann P, Hatta M, Feldmann F, Alimonti JB, Fernando L, Li Y, Katze MG, Feldmann H, Kawaoka Y. Aberrant innate immune response in lethal infection of macaques with the 1918 influenza virus. Nature. 2007; 445:319–323. [PubMed: 17230189]
57. Kim HM, Lee YW, Lee KJ, Kim HS, Cho SW, van Rooijen N, Guan Y, Seo SH. Alveolar macrophages are indispensable for controlling influenza viruses in lungs of pigs. J Virol. 2008; 82:4265–4274. [PubMed: 18287245]
58. Purnama C, Ng SL, Tetlak P, Setiagani YA, Kandasamy M, Baalasubramanian S, Karjalainen K, Ruedl C. Transient ablation of alveolar macrophages leads to massive pathology of influenza infection without affecting cellular adaptive immunity. Eur J Immunol. 2014; 44:2003–2012. [PubMed: 24687623]
59. Tate MD, Pickett DL, van Rooijen N, Brooks AG, Reading PC. Critical role of airway macrophages in modulating disease severity during influenza virus infection of mice. J Virol. 2010; 84:7569–7580. [PubMed: 20504924]
60. Belge KU, Dayyani F, Horelt A, Siedlar M, Frankenberger M, Frankenberger B, Espevik T, Ziegler-Heitbrock L. The proinflammatory CD14+CD16+DR++ monocytes are a major source of TNF. J Immunol. 2002; 168:3536–3542. [PubMed: 11907116]
61. Herold S, von Wulffen W, Steinmueller M, Pleschka S, Kuziel WA, Mack M, Srivastava M, Seeger W, Maus UA, Lohmeyer J. Alveolar epithelial cells direct monocyte transepithelial migration upon influenza virus infection: impact of chemokines and adhesion molecules. J Immunol. 2006; 177:1817–1824. [PubMed: 16849492]
62. Herold S, Steinmueller M, von Wulffen W, Cakarova L, Pinto R, Pleschka S, Mack M, Kuziel WA, Corazza N, Brunner T, Seeger W, Lohmeyer J. Lung epithelial apoptosis in influenza virus pneumonia: the role of macrophage-expressed TNF-related apoptosis-inducing ligand. J Exp Med. 2008; 205:3065–3077. [PubMed: 19064696]
63. Hogner K, Wolff T, Pleschka S, Plog S, Gruber AD, Kalinke U, Walmrath HD, Bodner J, Gattenlohner S, Lewe-Schlosser P, Matrosovich M, Seeger W, Lohmeyer J, Herold S.

Macrophage-expressed IFN-beta contributes to apoptotic alveolar epithelial cell injury in severe influenza virus pneumonia. PLoS Pathog. 2013; 9:e1003188. [PubMed: 23468627]

64. Aldridge JR Jr, Moseley CE, Boltz DA, Negovetich NJ, Reynolds C, Franks J, Brown SA, Doherty PC, Webster RG, Thomas PG. TNF/iNOS-producing dendritic cells are the necessary evil of lethal influenza virus infection. Proc Natl Acad Sci U S A. 2009; 106:5306–5311. [PubMed: 19279209]
65. Lin KL, Suzuki Y, Nakano H, Ramsburg E, Gunn MD. CCR2+ monocyte-derived dendritic cells and exudate macrophages produce influenza-induced pulmonary immune pathology and mortality. J Immunol. 2008; 180:2562–2572. [PubMed: 18250467]
66. Kumagai Y, Takeuchi O, Kato H, Kumar H, Matsui K, Morii E, Aozasa K, Kawai T, Akira S. Alveolar macrophages are the primary interferon-alpha producer in pulmonary infection with RNA viruses. Immunity. 2007; 27:240–252. [PubMed: 17723216]
67. Menachery VD, Eisfeld AJ, Schafer A, Josset L, Sims AC, Proll S, Fan S, Li C, Neumann G, Tilton SC, Chang J, Gralinski LE, Long C, Green R, Williams CM, Weiss J, Matzke MM, Webb-Robertson BJ, Schepmoes AA, Shukla AK, Metz TO, Smith RD, Waters KM, Katze MG, Kawaoka Y, Baric RS. Pathogenic influenza viruses and coronaviruses utilize similar and contrasting approaches to control interferon-stimulated gene responses. mBio. 2014; 5:e01174–01114. [PubMed: 24846384]
68. Itoh Y, Shinya K, Kiso M, Watanabe T, Sakoda Y, Hatta M, Muramoto Y, Tamura D, Sakai-Tagawa Y, Noda T, Sakabe S, Imai M, Hatta Y, Watanabe S, Li C, Yamada S, Fujii K, Murakami S, Imai H, Kakugawa S, Ito M, Takano R, Iwatsuki-Horimoto K, Shimojima M, Horimoto T, Goto H, Takahashi K, Makino A, Ishigaki H, Nakayama M, Okamatsu M, Takahashi K, Warshauer D, Shult PA, Saito R, Suzuki H, Furuta Y, Yamashita M, Mitamura K, Nakano K, Nakamura M, Brockman-Schneider R, Mitamura H, Yamazaki M, Sugaya N, Suresh M, Ozawa M, Neumann G, Gern J, Kida H, Ogasawara K, Kawaoka Y. In vitro and in vivo characterization of new swine-origin H1N1 influenza viruses. Nature. 2009; 460:1021–1025. [PubMed: 19672242]
69. Skinner JA, Zurawski SM, Sugimoto C, Vinet-Oliphant H, Vinod P, Xue Y, Russell-Lodrigue K, Albrecht RA, Garcia-Sastre A, Salazar AM, Roy CJ, Kuroda MJ, Oh S, Zurawski G. Immunologic characterization of a rhesus macaque H1N1 challenge model for candidate influenza virus vaccine assessment. Clin Vaccine Immunol. 2014; 21:1668–1680. [PubMed: 25298110]

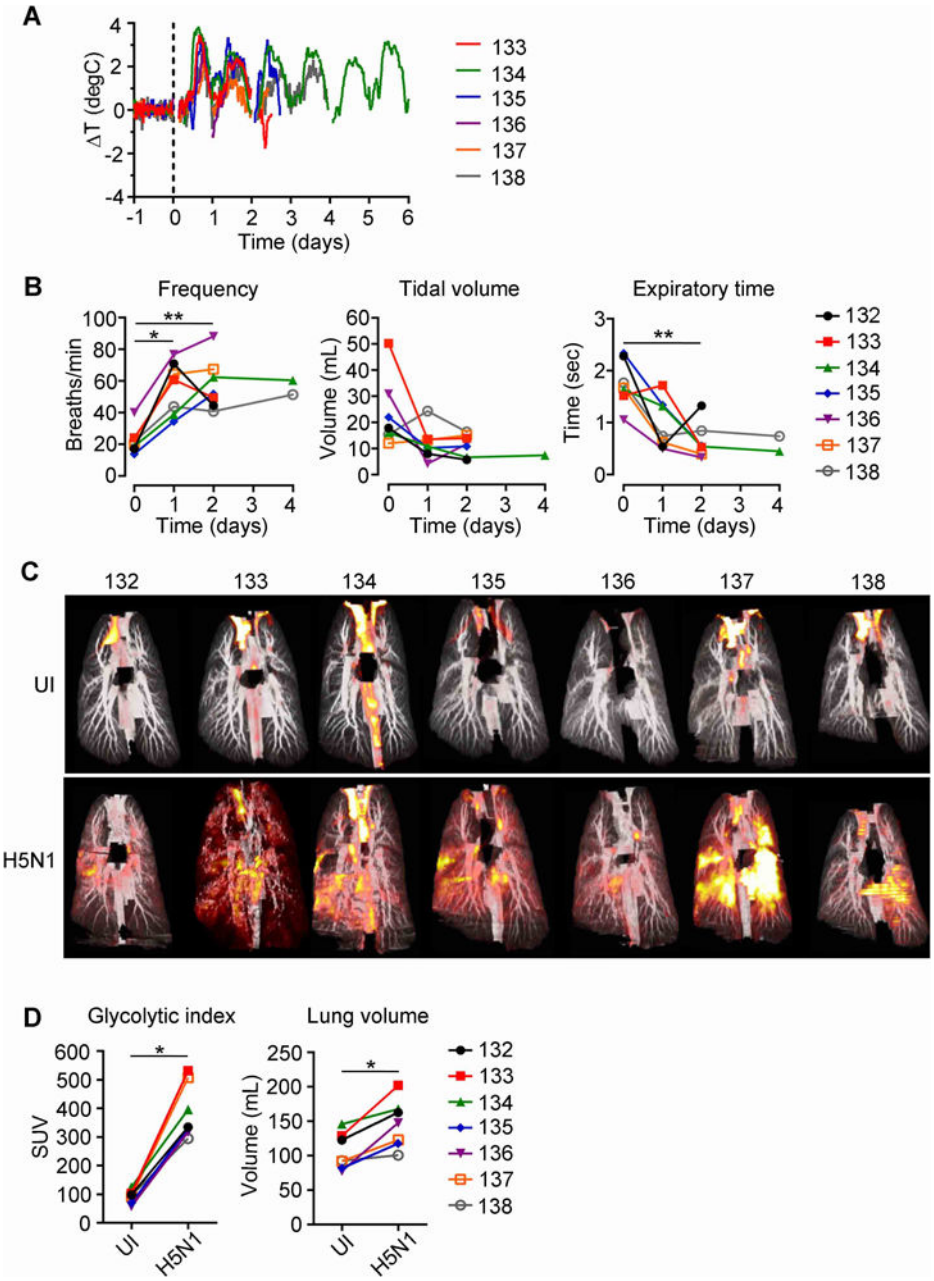

FIGURE 1.

Aerosolized H5N1 infection of macaques produces fulminant bilateral pneumonia. (**A**) Residual temperature differences relative to pre-infection baseline values determined by radiotelemetry. (**B**) Respiratory rate, tidal volume and expiratory time following H5N1 infection measured by plethysmography. (**C**) Paired combined PET-CT images from each animal taken prior to infection (UI) and at 2 days after H5N1 infection. Red coloration indicates FDG uptake. (**D**) Quantification of lung FDG uptake measured as standardized uptake value (SUV) and of lung volume before and at 2 days after H5N1 infection. *P* values were determined through Friedman tests, followed by Dunn's multiple comparisons tests (**B**) and Wilcoxon matched-pairs signed rank test (**D**). * $P<0.05$, ** $P<0.01$.

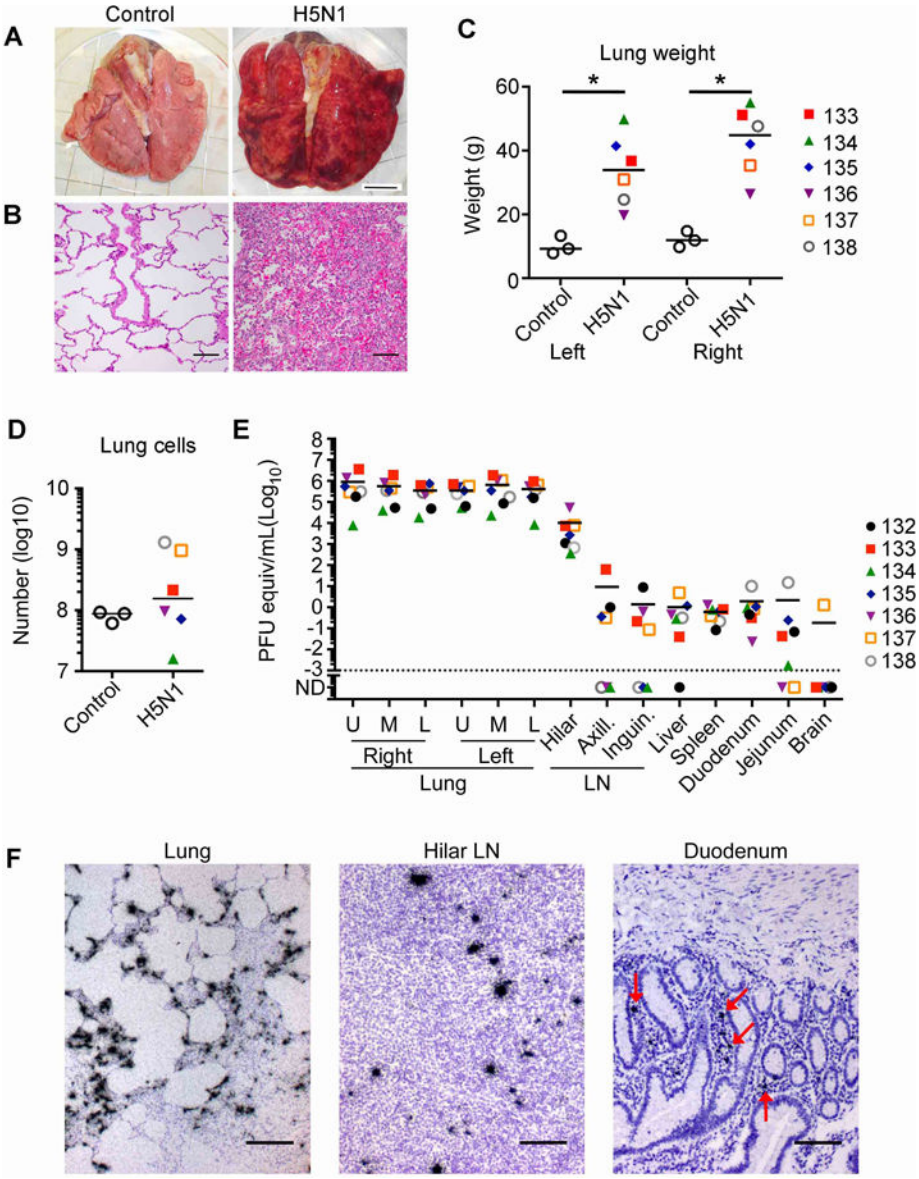

FIGURE 2.

Profound lung inflammation and systemic infection following aerosolized H5N1 virus exposure. (**A**) Lungs from an uninfected control and H5N1 infected macaque. Scale bar = 2 cm. (**B**) H&E staining of control and H5N1 infected lungs at day 2 PI. Scale bar = 100 um. (**C**) Lung weights at necropsy. (**D**) Total number of cells yielded from enzymatic digestion of lungs. (**E**) Semi-quantitative real-time RT-PCR of influenza virus in homogenized tissues. ND, not detected. (**F**) *In situ* hybridization of paraffin-embedded sections from upper lung, hilar lymph node and duodenum at day 2 PI. Influenza virus RNA is seen as dark grains in the walls of most alveoli, in the lymph node paracortex and duodenum lamina propria (red arrows). Counterstaining of lung sections reveals fluid accumulation in alveolar spaces. Scale bar = 100 μm. Horizontal lines in graphs represent medians. *P* values were determined through Mann-Whitney *U* tests. * $P < 0.05$.

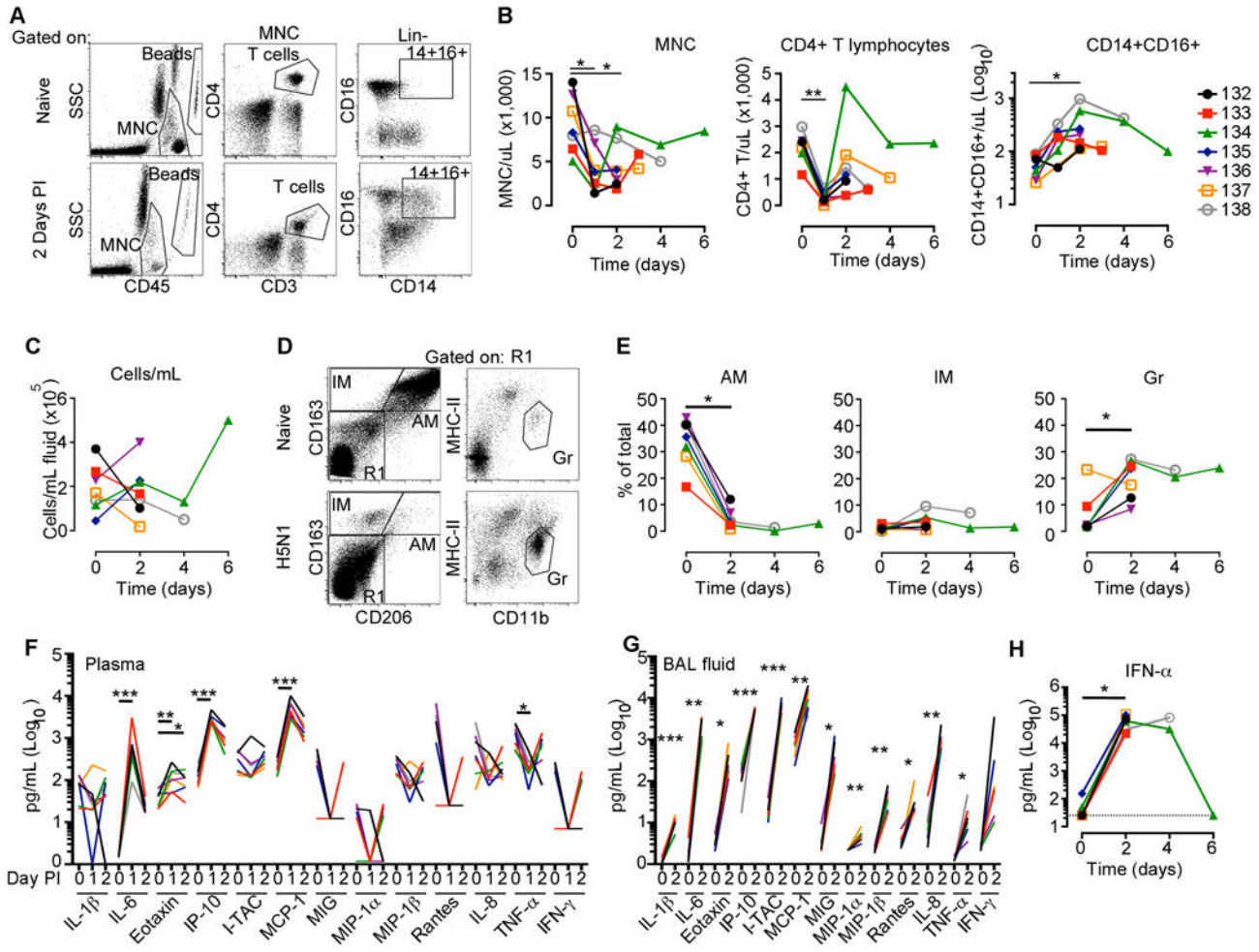

FIGURE 3.

Innate immune response in blood and BAL following aerosolized H5N1 virus infection. (**A**) Gating strategy to identify blood mononuclear cells (MNC, $CD45^+$), $CD4^+$ T lymphocytes (T cells, $CD45^+CD3^+CD4^+$), and intermediate monocytes ($CD45^+CD3^-CD20^-HLA\text{-}DR^+CD14^+CD16^+$) by flow cytometry. (**B**) Quantification of MNC, $CD4^+$ T lymphocytes and intermediate monocytes ($CD14^+CD16^+$) in blood. (**C**) Quantitation of cells in BAL fluid. (**D**) Gating strategy to identify alveolar macrophages (AM, $CD163^+CD206^+$), interstitial macrophages (IM, $CD163^+CD206^-$), and granulocytes (Gr, $CD163^-CD206^-CD11b^+HLA\text{-}DR^-$) in BAL fluid by flow cytometry. (**E**) Quantification of AM, IM, and Gr in BAL samples. (**F**) Cytokine concentrations measured in the plasma and (**G**) BAL fluid through flow cytometric cytokine bead array. (**H**) IFN-α2 concentrations in BAL fluid as measured by ELISA. *P* values were determined through Friedman tests, followed by Dunn's multiple comparisons tests (**B**, **F**), Wilcoxon matched-pairs signed rank test (**E**, **H**), and a paired t test (**G**). * $P<0.05$, ** $P<0.01$, *** $P<0.001$.

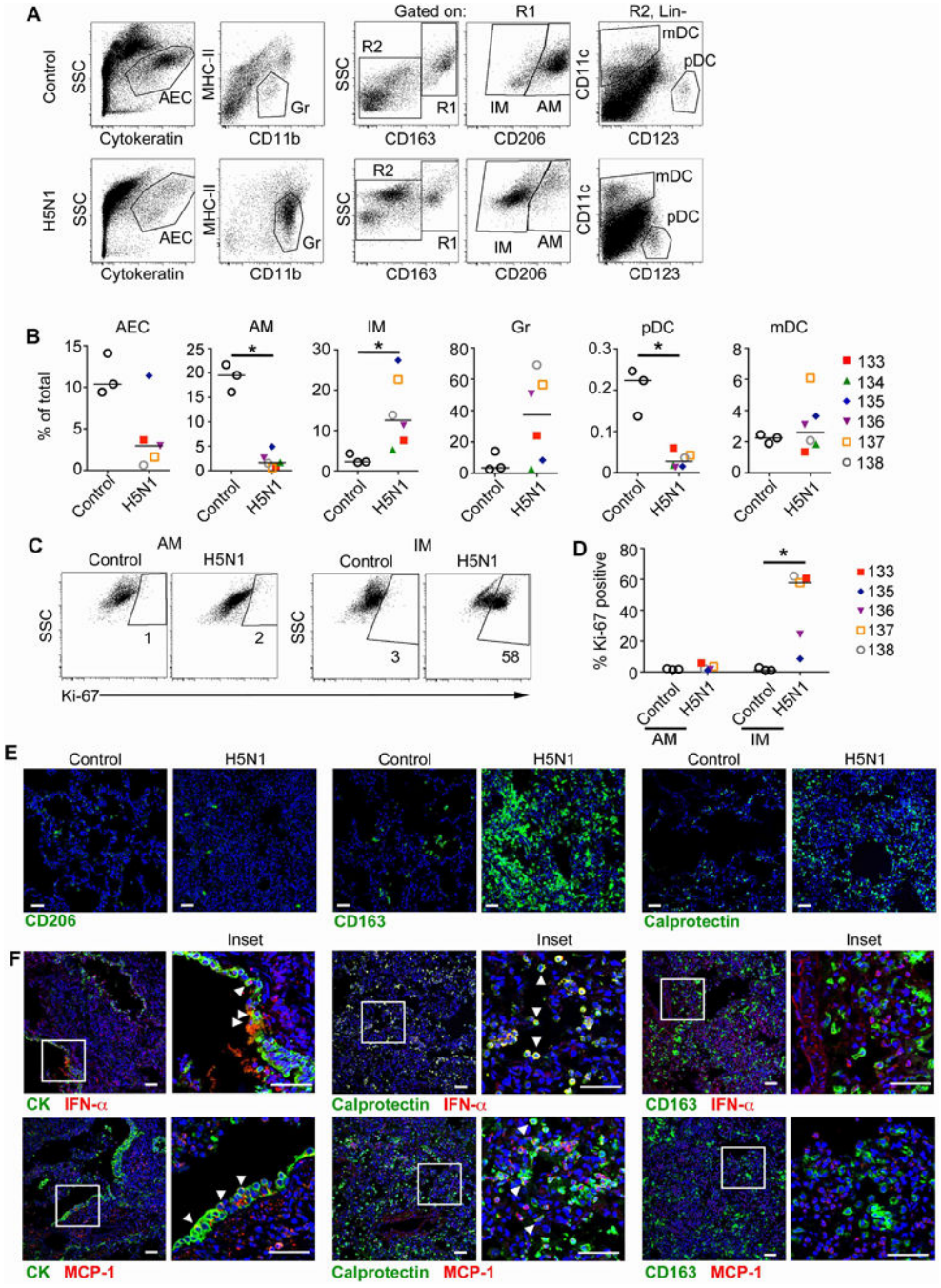

FIGURE 4.

H5N1 infection leads to decimation of alveolar macrophages and infiltration of interstitial macrophages and neutrophils. (**A**) Gating strategy to identify alveolar epithelial cells (AEC, cytokeratin^{+}), neutrophils (Gr, CD11b^{+}HLA-DR^{-}), alveolar macrophages (AM, CD163^{+}CD206^{+}), interstitial macrophages (IM, CD163^{+}CD206^{-}), plasmacytoid dendritic cells (pDC, Lin^{-} (CD3/CD20)HLA-DR^{+}CD163^{-}CD123^{+}), and myeloid dendritic cells (mDC, Lin^{-} (CD3/CD20)HLA-DR^{+}CD163^{-}CD11c^{+}) in lung suspensions by flow cytometry. (**B**) Quantification of AEC, Gr, AM, IM, pDC, and mDC in lung suspensions.

(**C**) Ki-67 staining in alveolar macrophages and interstitial macrophages as measured through flow cytometry. Numbers represent the percentage of each cell type expressing Ki-67. (**D**) Quantification of Ki-67 expression on alveolar and interstitial macrophages. (**E**) Immunofluorescence staining of lung sections from control and H5N1 infected macaques using the indicated antibodies. Scale bar = 50 um. (**F**) Lung sections stained with antibodies to cytokeratin (identifying AEC), calprotectin (neutrophils), and CD163 (interstitial macrophages) and either IFN-α (top panels) or MCP-1 (bottom panels). Arrowheads indicate cells co-stained for cellular markers and cytokines. Scale = 50 um. Horizontal lines in graphs represent medians. *P* values were determined through Mann-Whitney *U* tests. * $P < 0.05$.

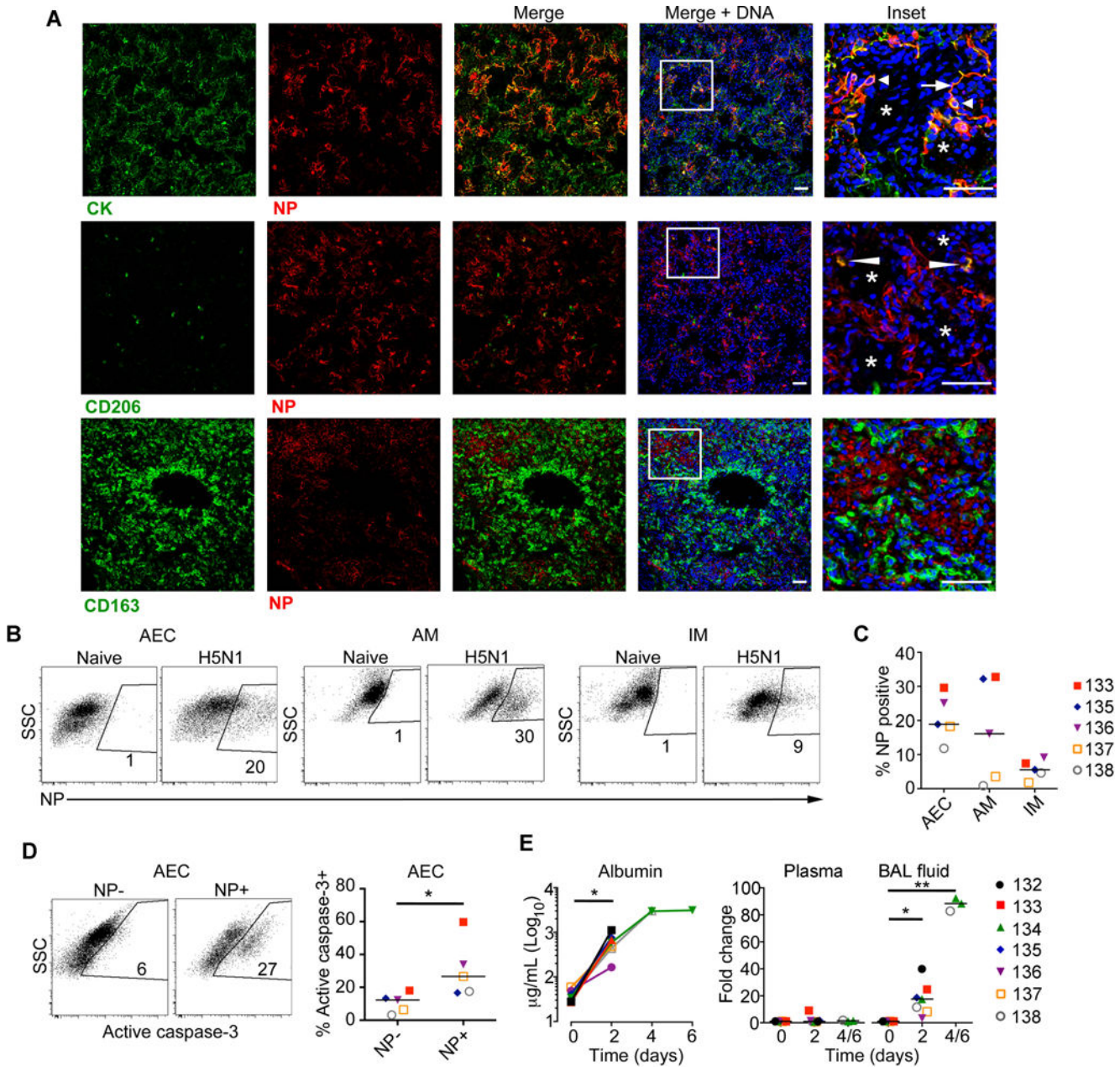

FIGURE 5.

H5N1 infects AEC and alveolar macrophages and causes plasma leakage into airways. (**A**) Lung sections co-stained with antibodies to cytokeratin (CK), CD206, or CD163 and H5N1 nucleoprotein (NP). Arrow indicates infected type I pneumocytes and arrowhead indicates infected type II pneumocytes. Narrow arrowhead indicates infected alveolar macrophages. White asterisks mark alveolar spaces containing nucleated cells, identified by blue staining. Scale bar = 50 um. (**B**) Flow cytometric analysis of nucleoprotein expression in alveolar epithelial cells (AEC), alveolar macrophages (AM), and interstitial macrophages (IM) in naïve or H5N1 infected lung. Numbers represent percentage of each cell type expressing nucleoprotein. Gating is based on staining of naïve samples stained for H5N1. (**C**)

Quantification of nucleoprotein^{+} AEC, AM, and IM. (**D**) Flow cytometric analysis of active caspase-3 expression in AEC from an infected macaque co-stained for nucleoprotein expression. (**E**) Albumin concentration in BAL fluid and fold increase in albumin concentration relative to pre-infection concentrations in plasma and BAL fluid. Horizontal lines in graphs represent medians. *P* value was determined through Wilcoxon matched-pairs signed rank test (**D**, **E**) and a Kruskal-Wallis test followed by a Dunn's multiple comparisons test (**E**). * $P<0.05$, ** $P<0.01$.

Table I

Characteristics of infection and virus titers

			Virus titer (log_{10} pfu/ml or pfu/g)												
			Nasal wash				BAL			Left lung			Right lung		
Animal ID	Virus dose (log_{10} pfu)	Time to death (days)	d1	d2	d4	d6	d2	d4	d6	Upper	Middle	Lower	Upper	Middle	Lower
132	7.26	3	0.70	0	–	–	3.04	–	–	3.73	4.33	4.25	4.23	4.36	4.79
133	7.17	2*	1.81	1.00	–	–	4.03	–	–	7.26	6.64	6.79	6.73	4.60	7.80
134	7.07	6*	1.40	3.18	1.00	0	7.45	5.13	4.96	6.69	5.77	3.00	5.72	6.03	3.65
135	6.16	3	2.05	3.81	–	–	3.10	–	–	5.39	5.56	5.75	5.56	5.77	5.85
136	6.46	2*	0	0	–	–	3.47	–	–	5.86	5.66	5.29	5.36	5.91	4.98
137	6.37	2*	0	0	–	–	3.63	–	–	5.29	5.73	5.64	5.66	5.76	5.61
138	6.57	4	0	0.48	0	–	3.33	3.67	–	4.57	5.23	5.51	4.85	5.37	4.20
Mean	6.72	3.2	0.85	1.21	0.50	0	4.01	4.40	4.96	5.54	5.56	5.18	5.44	5.40	5.27

*Humanely sacrificed